MATHEMATICAL METHODS IN THE APPLIED SCIENCES
Math. Meth. Appl. Sci. 2005; **28**:881–901
Published online 29 November 2004 in Wiley InterScience (www.interscience.wiley.com). DOI: 10.1002/mma.593
MOS subject classification: 47 J 40; 49 J 40; 74 C 05

A quasi-static boundary value problem in multi-surface elastoplasticity: part 2—numerical solution

Martin Brokate[1,‡], Carsten Carstensen[2,§] and Jan Valdman[3,*,†]

[1]*Zentrum Mathematik, TU Munich, Boltzmannstrasse 3, D-85747 Garching, Germany*
[2]*Department of Mathematics, Humboldt-Universität zu Berlin, Unter den Linden 6, D-10099 Berlin, Germany*
[3]*Special Research Program SFB F013 'Numerical and Symbolic Scientific Computing', Johannes Kepler University Linz, Altenbergerstrasse 69, A-4040 Linz, Austria*

SUMMARY

Multi-yield elastoplasticity models a material with more than one plastic state and hence allows for refined approximation of irreversible deformations. Aspects of the mathematical modelling and a proof of unique existence of weak solutions can be found in part I of this paper (*Math. Models Methods Appl. Sci.* 2004). In this part II we establish a canonical time–space discretization of the evolution problem and present various algorithms for the solving really discrete problems. Based on a global Newton–Raphson solver, we carefully study and solve elementwise inner iterations. Numerical examples illustrate the model and its flexibility to allow for refined hysteresis curves. Copyright © 2005 John Wiley & Sons, Ltd.

KEY WORDS: variational inequalities; elastoplasticity; phase transition multi-surface model; multi-yield Prandtl–Ishlinskii model; hysteresis; finite element method

1. INTRODUCTION

In this article we consider the quasi-static initial-boundary value problem for small strain elastoplasticity with a multi-surface constitutive law of linear kinematic hardening type. In the first part [1], we presented the precise formulation of the initial-boundary value problem in the form of a system of evolution variational inequalities for unknown fields of displacement

*Correspondence to: Jan Valdman, Special Research Program SFB F013 'Numerical and Symbolic Scientific Computing', Johannes Kepler University Linz, Altenbergerstrasse 69, A-4040 Linz, Austria.
†E-mail: jan.valdman@sfb013.uni-linz.ac.at
‡E-mail: brokate@ma.tum.de
§E-mail: cc@math.hu-berlin.de

Contract/grant sponsor: German Research Foundation
Contract/grant sponsor: Forschungszentrum FZ86
Contract/grant sponsor: Austrian Science Fund; contract/grant number: SFB F013/F1306

 Received 16 September 2003

and several plastic strain components attached to different surfaces. We proved the existence and uniqueness of its solution by verifying the assumptions of a general theorem [2] and also derived an estimate for the ellipticity constant in dependence on the material parameters.

This second part concerns a time–space discretization of the system of variational inequalities presented in the first part, it develops a solution algorithm and reports on numerical examples in 2D and 3D. For the numerical treatment of single-yield hardening models described by a single variational inequality we refer to Reference [3]. In those works, we use the conforming finite element space of lowest order with elementwise linear displacement and constant plastic strains. In order to describe the multi-yield aspect in a compact way, a matrix formulation is used and original system of inequalities is rewritten as an equilibrium equation and an elementwise matrix inequality for plastic strains only. Then, an algorithm with an outer Newton–Raphson method for solving the equilibrium equation is applied. An inner loop for elementwise solution of the matrix inequality is carefully studied. It has already been shown that a solution of the elementwise inequality can be written explicitly in the single-yield case. Our analysis indicates that, already in the two-yield case, the situation is considerably more difficult. Indeed, one encounters root finding of a 8th degree polynomial. Alternatively, we derive an iterative algorithm for the original matrix inequality and prove its geometrical convergence.

Numerical experiments demonstrate the feasibility of the algorithm; the different hysteresis behaviour curves and elastoplastic zones and their evolution is shown. An illustrating movie for a time-evolving elastoplastic process can be downloaded from the web [4].

The paper is organized as follows. Section 2 briefly recalls the mathematical formulation from part I and then establishes the discrete model. The Newton–Raphson method of Section 3 allows for an effective solution of the non-linear system of variational equations with an outer and an elementwise inner loop. Numerical examples in Section 4 illustrate the behaviour of the proposed refined two-yield elastoplastic model.

2. MATHEMATICAL AND DISCRETE MODEL

Following the first part of this article [1] the multi-yield elastoplastic continuum can be modelled by the following abstract evolution variational inequality explained below in detail.

Problem 2.1 (*BVP of quasi-static multi-surface elastoplasticity*)
Given $\ell \in H^1(0,T;\mathscr{H}^*)$ with $\ell(0)=0$ in a Hilbert space $\mathscr{H}$ and its dual $\mathscr{H}^*$ and duality bracket $\langle\cdot,\cdot\rangle$, find $x \in H^1(0,T;\mathscr{H})$ with $x(0)=0$ such that

$$\langle \ell(t), y-\dot{x}(t)\rangle \leqslant a(x(t), y-\dot{x}(t)) + \psi(y) - \psi(\dot{x}(t)) \quad \textit{for all } \ y \in \mathscr{H} \tag{1}$$

holds for almost all $t \in (0,T)$.

Therein, we are given $x=(u,(p_r)_{r\in I}), y=(v,(q_r)_{r\in I})$ in $\mathscr{H}=H^1_D(\Omega)\times\Pi_{r\in I}\operatorname{dev}(L^2(\Omega)^{d\times d}_{\mathrm{sym}})$ with

$$H^1_D(\Omega)=\{v\in H^1(\Omega)^d \,|\, v=0 \text{ on } \Gamma_D\}$$

$$\operatorname{dev}(L^2(\Omega)^{d\times d}_{\mathrm{sym}})=\{q\in L^2(\Omega)^{d\times d}\colon \text{ for all } x\in\Omega, q(x)\in \operatorname{dev}\mathbb{R}^{d\times d}_{\mathrm{sym}}\}$$

for the usual Sobolev and Lebesgue spaces $H^1(\Omega)$ and $L^2(\Omega)$ on the bounded Lipschitz domain Ω (which has a polygonal boundary Γ split into a Dirichlet Γ_D and Neumann $\Gamma_N := \Gamma \backslash \Gamma_D$ parts), $\operatorname{dev} \mathbb{R}^{d\times d}_{\mathrm{sym}}$ is defined using the deviatoric operator dev: $\mathbb{R}^{d\times d}_{\mathrm{sym}} \to \mathbb{R}^{d\times d}_{\mathrm{sym}}$, $\operatorname{dev} q = q - (1/d)\operatorname{tr} q\, \mathbb{I}$ by

$$\operatorname{dev} \mathbb{R}^{d\times d}_{\mathrm{sym}} = \{q \in \mathbb{R}^{d\times d}_{\mathrm{sym}} : \exists_p \in \mathbb{R}^{d\times d}_{\mathrm{sym}}, q = \operatorname{dev} p\}$$

Here and below, $\mathbb{I}$ denotes the identity tensor (an identity matrix) and $\operatorname{tr} : \mathbb{R}^{d\times d} \to \mathbb{R}$ defines the trace of a matrix, $\operatorname{tr} \varepsilon := \sum_{j=1}^{d} \varepsilon_{jj}$, for $\varepsilon \in \mathbb{R}^{d\times d}_{\mathrm{sym}}$, where d is the problem dimension. The bilinear form $a(\cdot,\cdot)$, the linear form $\ell(t)$, and the non-linear functional ψ read

$$\begin{aligned} a : \mathscr{H} \times \mathscr{H} \to \mathbb{R}, \quad a(x,y) &= \int_\Omega \mathbb{C}\left(\varepsilon(u) - \sum_{r\in I} p_r\right) : \left(\varepsilon(v) - \sum_{r\in I} q_r\right) \mathrm{d}x \\ &\quad + \sum_{r\in I} \int_\Omega \mathbb{H}_r p_r : q_r \,\mathrm{d}x \\ \ell(t) : \mathscr{H} \to \mathbb{R}, \quad \langle \ell(t), y\rangle &= \int_\Omega f(t)\cdot v \,\mathrm{d}x + \int_{\Gamma_N} g(t)\cdot v \,\mathrm{d}S(x) \qquad (2) \\ \psi : \mathscr{H} \to \mathbb{R}, \quad \psi(y) &= \sum_{r\in I} \int_\Omega \sigma_r^y |q_r| \,\mathrm{d}x \end{aligned}$$

Here and throughout the paper, $\varepsilon(v) := \operatorname{sym} Dv := \frac{1}{2}(Dv + (Dv)^{\mathrm{T}})$ denotes the linear Green strain and $A{:}B := \sum_{j,k=1}^{d} A_{jk}B_{jk}$ is the Euclid product of $A, B \in \mathbb{R}^{d\times d}$. The linear elasticity matrix $\mathbb{C}$ from the isotropic case is defined by

$$\mathbb{C}\varepsilon = 2\mu\varepsilon + \lambda(\operatorname{tr}\varepsilon)\mathbb{I}$$

for the (positive) Lamé coefficients μ and λ. The hardening matrices read $\mathbb{H}_r = h_r\mathbb{I}$, where $h_r > 0$ are hardening coefficients. According to the choice of the index set I we classify a single-yield case with $I = \{1\}$, a two-yield case with $I = \{1,2\}$ and a more general M-yield case with $I = \{1,\ldots,M\}$. Further details on the notation can be found in Reference [1]. This paper essentially contributes to the two-yield model, i.e. $M = 2$, unless stated differently.

The discretization of the variational inequality (1) consists of time and space discretizations. We discretize the continuous time interval $(0,T)$ by the discrete times $t_0,\ldots,t_N$ with

$$0 = t_0 < \tau_1 \leqslant t_1 < \tau_2 \leqslant t_2 < \cdots \leqslant t_{N-1} < \tau_N \leqslant t_N = T$$

with a time step $k_j = t_j - t_{j-1}, j = 1,\ldots,N$ and the polygonal domain $\Omega \subset \mathbb{R}^2$ by a regular triangulation $\mathscr{T}$ in triangles in the sense of Ciarlet [5], i.e. $\mathscr{T}$ is a finite partition of Ω into closed triangles; two distinct elements T_1 and T_2 are either disjoint, or $T_1 \cap T_2$ is a complete edge or a common node of both T_1 and T_2. In the first time step t_1, the time derivative $\dot{x}(t_1)$ is approximated by the backward Euler method as $\dot{X}^1 = (X^1 - X^0)/k_1$, where $X^0 = 0$. The Hilbert space $\mathscr{H}$ is approximated by the conforming finite element subspace

$$\mathscr{S} = \mathscr{S}^1_D(\mathscr{T}) \times \prod_{r\in I} \operatorname{dev}(\mathscr{S}^0(\mathscr{T})^{d\times d}_{\mathrm{sym}})$$

which is a product space of the space of $\mathscr{T}$-piecewise constant functions

$$\operatorname{dev}(\mathscr{S}^0(\mathscr{T})^{d\times d}_{\mathrm{sym}}) := \{a \in L^2(\Omega)^{d\times d} : \forall T \in \mathscr{T}, a|_T \in \operatorname{dev} \mathbb{R}^{d\times d}_{\mathrm{sym}}\}$$

and the set of $\mathscr{T}$-piecewise affine functions that are zero on Γ_D by

$$\mathscr{S}^1_D(\mathscr{T}) := \{v \in H^1_D(\Omega) : \forall T \in \mathscr{T}, v|_T \in \mathscr{P}_1(T)^d\}$$

($\mathscr{P}_1(T)$ denotes the affine functions on T.) We discretize the variational inequality (1) as follows. Find $X^1 = (U^1, (P^1_r)_{r\in I}) := (U^1, P^1) \in \mathscr{S}$ such that, for all $Y = (V, (Q_r)_{r\in I}) := (V, Q) \in \mathscr{S}$,

$$\left\langle \ell(t_1), \left(Y - \frac{X^1 - X^0}{k_1}\right)\right\rangle \leqslant a\left(X^1, Y - \frac{X^1 - X^0}{k_1}\right) + \psi(Q) - \psi\left(\frac{P^1 - P^0}{k_1}\right)$$

After introducing an incremental variable $X := (U, P) = X^1 - X^0$ and a linear functional $L(Y) = \langle \ell(t_1), Y\rangle - a(X^0, Y)$ we obtain a one-time step discrete problem.

Lemma 1 (*equivalent reformulations*)
For each $X = (U, P) \in \mathscr{S}$ the following three conditions (a)–(c) are equivalent:

(a) $L(Y - X) \leqslant a(X, Y - X) + \psi(Q) - \psi(P)$ for all $Y = (V, Q) \in \mathscr{S}$.
(b) $\Phi(X) = \min_{Y\in\mathscr{S}} \Phi(Y)$ for $\Phi(Y) = \frac{1}{2}a(Y, Y) + \psi(Q) - L(Y)$.
(c) $L(Y - X) = a(X, Y - X)$ for all $Y = (V, P) \in \mathscr{S}$ and
$L(Y - X) \leqslant a(X, Y - X) + \psi(Q) - \psi(P)$ for all $Y = (U, Q) \in \mathscr{S}$.

Proof
Elementary calculations with the quadratic forms, we omit the details. □

The following matrix notation allows for a brief formulation of the discrete problem. Let

$$P := \begin{pmatrix} P_1 \\ \vdots \\ P_M \end{pmatrix}, \quad P^0 := \begin{pmatrix} P^0_1 \\ \vdots \\ P^0_M \end{pmatrix}, \quad Q := \begin{pmatrix} Q_1 \\ \vdots \\ Q_M \end{pmatrix}, \quad \hat{\Sigma} := \begin{pmatrix} \mathbb{C}\varepsilon(U) \\ \vdots \\ \mathbb{C}\varepsilon(U) \end{pmatrix}$$

$$\hat{\Sigma}^0 := \begin{pmatrix} \mathbb{C}\varepsilon(U^0) \\ \vdots \\ \mathbb{C}\varepsilon(U^0) \end{pmatrix}, \quad \hat{\mathbb{C}} := \begin{pmatrix} \mathbb{C} & \dots & \mathbb{C} \\ \vdots & & \vdots \\ \mathbb{C} & \dots & \mathbb{C} \end{pmatrix}, \quad \hat{\mathbb{H}} := \begin{pmatrix} \mathbb{H}_1 & \dots & 0 \\ \vdots & & \vdots \\ 0 & \dots & \mathbb{H}_M \end{pmatrix}$$

Since the plastic yield parameters $\sigma^y_1, \dots, \sigma^y_M$ are positive, the expansion

$$|(P_1, \dots, P_M)^{\mathrm{T}}|_{\sigma^y} := \sigma^y_1|P_1| + \cdots + \sigma^y_M|P_M|$$

defines a norm in $\mathbb{R}^{Md\times d}$, where $|\cdot|$ denotes the Frobenius norm. Then there holds

$$-a(X, Y-X) = \int_\Omega (\hat{\Sigma} - (\hat{\mathbb{C}} + \hat{\mathbb{H}})P) : (Q-P)\,\mathrm{d}x$$

$$L(Y-X) = \int_\Omega (\hat{\Sigma}^0 - (\hat{\mathbb{C}} + \hat{\mathbb{H}})P^0) : (Q-P)\,\mathrm{d}x$$

$$\psi(Y) = \int_\Omega |Q|_{\sigma^y}\,\mathrm{d}x$$

With the substitution $\hat{A} := \hat{\Sigma} + \hat{\Sigma}^0 - (\hat{\mathbb{C}} + \hat{\mathbb{H}})P^0$ and for $U = V$, inequality (c) from Lemma 1 reads

$$\int_\Omega (\hat{A} - (\hat{\mathbb{C}} + \hat{\mathbb{H}})P) : (Q-P)\,\mathrm{d}x \leqslant \int_\Omega (|Q|_{\sigma^y} - |P|_{\sigma^y})\,\mathrm{d}x \tag{3}$$

for all $Q \in \prod_{r=1}^{M} \mathrm{dev}(\mathscr{S}^0(\mathscr{T})^{d\times d}_{\mathrm{sym}})$. Owing to the zero-order discretization, P and $\hat{A}$ are constant matrices on every triangle T of the triangulation $\mathscr{T}$. It enables us to decompose inequality (3) elementwise. Given $\hat{A}, \hat{\mathbb{C}}, \hat{\mathbb{H}} \in \mathbb{R}^{Md\times Md}$, we seek $P = (P_1, \ldots, P_M)^{\mathrm{T}} \in \mathbb{R}^{Md\times d}$ with $P_1, \ldots, P_M \in \mathrm{dev}\,\mathbb{R}^{d\times d}_{\mathrm{sym}}$, such that for all $Q = (Q_1, \ldots, Q_M)^{\mathrm{T}} \in \mathbb{R}^{Md\times d}$ with $Q_1, \ldots, Q_M \in \mathrm{dev}\,\mathbb{R}^{d\times d}_{\mathrm{sym}}$ holds

$$(\hat{A} - (\hat{\mathbb{C}} + \hat{\mathbb{H}})P) : (Q-P) \leqslant |Q|_{\sigma^y} - |P|_{\sigma^y} \tag{4}$$

Detailed formulation of the equilibrium equation together with the latter inequality define the discrete problem:

Problem 2.2 (*discrete problem*)
Given $U^0 \in \mathscr{S}^1_D(\mathscr{T})$, $P^0_1, \ldots, P^0_M \in \mathrm{dev}(\mathscr{S}^0(\mathscr{T})^{d\times d}_{\mathrm{sym}})$, seek $U^1 \in \mathscr{S}^1_D(\mathscr{T})$ such that for all $V \in \mathscr{S}^1_D(\mathscr{T})$,

$$\int_\Omega \mathbb{C}\left(\varepsilon(U^1) - \sum_{r=1}^{M} P^1_r\right) : \varepsilon(V)\,\mathrm{d}x - \int_\Omega f(t)V\,\mathrm{d}x - \int_{\Gamma_N} gV\,\mathrm{d}x = 0 \tag{5}$$

Here $P = (P_1, \ldots, P_M)^{\mathrm{T}} = (P^1_1, \ldots, P^1_M)^{\mathrm{T}} - (P^0_1, \ldots, P^0_M)^{\mathrm{T}}$ satisfies elementwise the inequality

$$(\hat{A} - (\hat{\mathbb{C}} + \hat{\mathbb{H}})P) : (Q-P) \leqslant |Q|_{\sigma^y} - |P|_{\sigma^y} \tag{6}$$

for all $Q = (Q_1, \ldots, Q_M)^{\mathrm{T}}$ with $Q_1, \ldots, Q_M \in \mathrm{dev}(\mathscr{S}^0(\mathscr{T})^{d\times d}_{\mathrm{sym}})$.

3. NUMERICAL SOLUTION OF DISCRETE MODEL

The numerical solution of the discrete problem for $d = 2$ is discussed in this and the subsequent section for it is split into an outer and an inner iteration.

3.1. Outer loop in Newton–Raphson scheme

Equilibrium equation (5) represents a non-linear system of equations for unknown displacements and plastic strains. As it is explained later in Sections 3.2 and 3.3 for cases of single- and two-yield models, the plastic strains can be calculated from displacements elementwise by solving inequality (6). Therefore, for the triangulation $\mathscr{T}$ with N nodes in $d=2$ dimensions, the equilibrium equation (5) together with inequality (6) can be equivalently understood as a non-linear system of equations for $2N$ displacement unknowns $\mathbf{U}^1=(U_1^1,\ldots,U_{2N}^1)^{\mathrm{T}}$ written in an abstract form as

$$\mathbf{F}_i(\mathbf{U}^1)=0 \quad \text{for all } i=1,\ldots,2N \tag{7}$$

We use the Newton–Raphson method for the iterative solution of (7).

Algorithm 3.1 (*Newton–Raphson method*)

(a) Choose an initial approximation $\mathbf{U}_0^1\in\mathbb{R}^{2\mathbf{N}}$, set $k:=0$.
(b) Let $k:=k+1$, solve $\mathbf{U}_\mathbf{k}^1$ from $D\mathbf{F}(\mathbf{U}_{\mathbf{k}-1}^1)(\mathbf{U}_\mathbf{k}^1-\mathbf{U}_{\mathbf{k}-1}^1)=-\mathbf{F}(\mathbf{U}_{\mathbf{k}-1}^1)$.
(c) If $\mathbf{U}_\mathbf{k}^1-\mathbf{U}_{\mathbf{k}-1}^1$ is sufficiently small then output $\mathbf{U}_\mathbf{k}^1$, otherwise goto (b).

Remark 1
In order to incorporate the Dirichlet boundary conditions properly, the linear system in step (b) is extended,

$$\begin{pmatrix} D\mathbf{F}(\mathbf{U}_{\mathbf{k}-1}^1) & B^{\mathbf{T}} \\ B & 0 \end{pmatrix}\begin{pmatrix} \mathbf{U}_\mathbf{k}^1-\mathbf{U}_{\mathbf{k}-1}^1 \\ \lambda \end{pmatrix}=\begin{pmatrix} -\mathbf{F}(\mathbf{U}_{\mathbf{k}-1}^1) \\ 0 \end{pmatrix}$$

with some matrix B and the vector of Lagrange parameters λ, see Reference [6].

Remark 2
Here, $D\mathbf{F}(\mathbf{U}_\mathbf{k}^1)\in\mathbb{R}^{2N\times 2N}$ represents a sparse tangential stiffness matrix

$$D\mathbf{F}(\mathbf{U})_{ij}\approx\frac{\mathbf{F}(U_1,\ldots,U_j+\varepsilon_j,\ldots,U_{2N})_i-\mathbf{F}(U_1,\ldots,U_j-\varepsilon_j,\ldots,U_{2N})_i}{2\varepsilon_j}$$

approximated by a central difference scheme with small parameters $\varepsilon_j>0$, $j=1,\ldots,2N$.

Remark 3 (*Three stages convergence control*)
The termination criterion used in step (c) reads

$$\frac{|\mathbf{U}_\mathbf{k}^1-\mathbf{U}_{\mathbf{k}-1}^1|}{|\mathbf{U}_\mathbf{k}^1|+|\mathbf{U}_{\mathbf{k}-1}^1|}<\mathrm{tol} \quad \text{or } |\mathbf{U}_\mathbf{k}^1|+|\mathbf{U}_{\mathbf{k}-1}^1|=0$$

together with the condition $r_\mathbf{k}\geqslant r_{\mathbf{k}-1}$, where $r_\mathbf{k}=|\mathbf{F}(\mathbf{U}_\mathbf{k}^1)-B^{\mathrm{T}}\lambda|$ is a residual. If the number k of iterations exceeds some predefined bound, Algorithm 3.1 terminates with no solution.

Remark 4 (*Nested iterations*)
The nested iteration technique [7] is applied for the solution of the problem on nested meshes $\mathscr{T}_0\subseteq\mathscr{T}_1\subseteq\cdots\subseteq\mathscr{T}_F$.

3.2. Inner loop for single-yield model

The single-yield model is specified by one plastic strain $P \in \mathbb{R}^{2\times 2}_{\mathrm{sym}}$ with $\operatorname{tr} P = 0$, the elastic matrix $\mathbb{C}$ with $\mathbb{C}P = 2\mu P$, the hardening matrix $\mathbb{H}$ with $\mathbb{H}P = hP$, the matrix norm $|P|_{\sigma^y} = \sigma^y|P|$ and the matrix $A := \hat{A} := \mathbb{C}\varepsilon(U) + \mathbb{C}\varepsilon(U^0) - (\mathbb{C}+\mathbb{H})P^0$. In this case there exists a solution formula:

Lemma 2 (*Alberty et al.* [8])
Given $A \in \mathbb{R}^{d\times d}_{\mathrm{sym}}$ and $\sigma^y > 0$ there exists exactly one $P \in \operatorname{dev} \mathbb{R}^{d\times d}_{\mathrm{sym}}$ that satisfies

$$\{A - (\mathbb{C}+\mathbb{H})P\} : (Q-P) \leqslant \sigma^y\{|Q| - |P|\}$$

for all $Q \in \operatorname{dev} \mathbb{R}^{d\times d}_{\mathrm{sym}}$. This P is characterized as the minimizer of

$$\tfrac{1}{2}(\mathbb{C}+\mathbb{H})Q : Q - Q : A + \sigma^y|Q| \tag{8}$$

(amongst trace-free symmetric $d\times d$-matrices) and is given by

$$P = \frac{(|\operatorname{dev} A| - \sigma^y)_+}{2\mu + h}\,\frac{\operatorname{dev} A}{|\operatorname{dev} A|} \tag{9}$$

where $(\cdot)_+ := \max\{0,\cdot\}$ denotes the non-negative part. The minimal value of (8) (attained for P as in (9)) is $-\frac{1}{2}(|\operatorname{dev} A| - \sigma^y)^2_+/(2\mu+h)$. The non-negative part enters through the different elastic ($|\operatorname{dev} A| < \sigma^y$) and plastic ($|\operatorname{dev} A| \geqslant \sigma^y$) phases.

3.3. Inner loop for two-yield model

The two-yield model is specified by two plastic strains P_1, P_2 that are coupled in a generalized plastic strain $P = (P_1, P_2)^{\mathrm{T}}$. The generalized elasticity matrix and the generalized hardening matrices read

$$\hat{\mathbb{C}} := \begin{pmatrix} \mathbb{C} & \mathbb{C} \\ \mathbb{C} & \mathbb{C} \end{pmatrix} \quad \text{and} \quad \hat{\mathbb{H}} := \begin{pmatrix} \mathbb{H}_1 & 0 \\ 0 & \mathbb{H}_2 \end{pmatrix}$$

the generalized loading matrix reads

$$\hat{A} = \begin{pmatrix} A_1 \\ A_2 \end{pmatrix} = \begin{pmatrix} \mathbb{C}\varepsilon(U) \\ \mathbb{C}\varepsilon(U) \end{pmatrix} + \begin{pmatrix} \mathbb{C}\varepsilon(U^0) \\ \mathbb{C}\varepsilon(U^0) \end{pmatrix} - \begin{pmatrix} \mathbb{C}+\mathbb{H}_1 & \mathbb{C} \\ \mathbb{C} & \mathbb{C}+\mathbb{H}_2 \end{pmatrix} \begin{pmatrix} P_1^0 \\ P_2^0 \end{pmatrix}$$

and the matrix norm is defined by

$$|P|_{\sigma^y} = \sigma_1^y|P_1| + \sigma_2^y|P_2|$$

Lemma 3
Given $\hat{A} = (A_1, A_2)^{\mathrm{T}}, A_1, A_2 \in \mathbb{R}^{d\times d}_{\mathrm{sym}}$ there exists exactly one $P = (P_1, P_2)^{\mathrm{T}}$, $P_1, P_2 \in \operatorname{dev} \mathbb{R}^{d\times d}_{\mathrm{sym}}$ that satisfies

$$(\hat{A} - (\hat{\mathbb{C}} + \hat{\mathbb{H}})P) : (Q-P) \leqslant |Q|_{\sigma^y} - |P|_{\sigma^y} \tag{10}$$

for all $Q = (Q_1, Q_2)^{\mathrm{T}}$, $Q_1, Q_2 \in \operatorname{dev} \mathbb{R}^{d\times d}_{\mathrm{sym}}$. This P is characterized as the minimizer of

$$f(Q) = \tfrac{1}{2}(\hat{\mathbb{C}} + \hat{\mathbb{H}})Q : Q - Q : \hat{A} + |Q|_{\sigma^y} \tag{11}$$

(amongst trace-free symmetric $d\times d$ matrices Q_1, Q_2).

Proof
The equivalence of $f(P) = \min_Q f(Q)$ and (10) is obvious. The function $f(Q)$ is strictly convex, continuous in the space of all trace-free symmetric $d \times d$ matrices Q_1, Q_2. There holds $\lim_{|Q| \to \infty} f(Q) = +\infty$, and so it attains exactly one minimum. □

Remark 5
In the absence of the off-diagonal blocks in the matrix $\hat{\mathbb{C}} = \mathrm{diag}(\mathbb{C}, \mathbb{C})$, the minimization problem (11) could be separated into two independent minimization problems in P_1 and P_2. The solution would then read

$$P_j = \frac{(|\mathrm{dev}\, A_j| - \sigma_j^y)_+}{2\mu + h_j} \frac{\mathrm{dev}\, A_j}{|\mathrm{dev}\, A_j|} \quad \text{for } j = 1, 2$$

The presence of the off-diagonal blocks leads to solving a simultaneous system for P_1 and P_2 in the following sections.

3.4. Reduction to polynomial of degree 8 for two-yield model

In general, the elementwise inner loop leads to the computation of roots of a single non-linear equation.

Lemma 4
Let B be a unit ball at the point 0, $B := \{Q \in \mathbb{R}^{d \times d}_{\mathrm{sym}} : |Q| \leqslant 1\}$. Then the subdifferential of $|P|_{\sigma^y} = \sigma_1^y P_1 + \sigma_2^y P_2$, where $P = (P_1, P_2) \in \mathbb{R}^{d \times d} \times \mathbb{R}^{d \times d}$ has the following form:

$$\partial |\cdot|_{\sigma^y}(P) = \begin{cases} \sigma_1^y B \times \sigma_2^y B & \text{if } P_1 = P_2 = 0 \\ \left\{ \sigma_1^y \frac{P_1}{|P_1|} \right\} \times \sigma_2^y B & \text{if } P_1 \neq 0, P_2 = 0 \\ \sigma_1^y B \times \left\{ \sigma_2^y \frac{P_2}{|P_2|} \right\} & \text{if } P_1 = 0, P_2 \neq 0 \\ \left\{ \sigma_1^y \frac{P_1}{|P_1|} \right\} \times \left\{ \sigma_2^y \frac{P_2}{|P_2|} \right\} & \text{if } P_1 \neq 0, P_2 \neq 0 \end{cases}$$

Proof
By the definition, the convex function $|P|_{\sigma^y}$ is decomposed as two convex functions $\sigma_1^y |P_1|$ and $\sigma_2^y |P_2|$. Both functions have subdifferentials, namely

$$\partial(\sigma_1^y |P_1|)(P) = \begin{cases} \sigma_2^y B \times \{0\} & \text{if } P_1 = 0 \\ \left\{ \sigma_2^y \frac{P_2}{|P_2|} \right\} \times \{0\} & \text{if } P_1 \neq 0 \end{cases} \tag{12}$$

and

$$\partial(\sigma_2^y |P_2|)(P) = \begin{cases} \{0\} \times \sigma_1^y B & \text{if } P_2 = 0 \\ \{0\} \times \left\{ \sigma_2^y \frac{P_2}{|P_2|} \right\} & \text{if } P_2 \neq 0 \end{cases} \tag{13}$$

The convex functions $\sigma_1^y |P_1|$ and $\sigma_2^y |P_2|$, considered as functions of two variables P_1, P_2, are continuous at the point $P_1 = P_2 = 0$ in the space $\mathbb{R}^{d \times d}_{\mathrm{sym}} \times \mathbb{R}^{d \times d}_{\mathrm{sym}}$. Therefore, with some calculus

of convex analysis, one can prove

$$\partial(|P|_{\sigma^y}) = \partial(\sigma_1^y|P_1|) + \partial(\sigma_2^y|P_2|)$$

The combination of (12) and (13) concludes the proof. □

For trace-free arguments $P_i \in \operatorname{dev}\mathbb{R}^{d\times d}_{\mathrm{sym}}$ holds $A_i : P_i = \operatorname{dev} A_i : P_i$ and $\mathbb{C}P_i = 2\mu P_i$ for $i = 1, 2$ and inequality (10) can be rewritten as an inclusion

$$\begin{pmatrix} \operatorname{dev} A_1 \\ \operatorname{dev} A_2 \end{pmatrix} - \begin{pmatrix} (2\mu + h_1)\mathbb{I} & 2\mu\mathbb{I} \\ 2\mu\mathbb{I} & (2\mu + h_2)\mathbb{I} \end{pmatrix} \begin{pmatrix} P_1 \\ P_2 \end{pmatrix} \in (\partial|\cdot|_{\sigma^y}(P_1, P_2))^{\mathrm{T}} \tag{14}$$

Lemma 4 divides the analysis of (14) into four cases in dependence of the combination of the values of P_1 and P_2:

Case 1: $P_1 = P_2 = 0$ with the following equivalences:

$$P_1 = P_2 = 0 \Leftrightarrow |\operatorname{dev} A_1| \leqslant \sigma_1^y \text{ and } |\operatorname{dev} A_2| \leqslant \sigma_2^y$$

Case 2: $P_1 = 0$, $P_2 \neq 0$, which means

$$\begin{pmatrix} \operatorname{dev} A_1 \\ \operatorname{dev} A_2 \end{pmatrix} - \begin{pmatrix} (2\mu + h_1)\mathbb{I} & 2\mu\mathbb{I} \\ 2\mu\mathbb{I} & (2\mu + h_2)\mathbb{I} \end{pmatrix} \begin{pmatrix} 0 \\ P_2 \end{pmatrix} \in \begin{pmatrix} \sigma_1^y B \\ \left\{\sigma_2^y \frac{P_2}{|P_2|}\right\} \end{pmatrix}$$

We may write equivalently

$$\operatorname{dev} A_1 - 2\mu P_2 \in \sigma_1^y B \tag{15}$$

$$\operatorname{dev} A_2 - (2\mu + h_2)P_2 = \sigma_2^y \frac{P_2}{|P_2|} \tag{16}$$

Elimination of P_2 from (16) yields

$$P_2 = \frac{|\operatorname{dev} A_2| - \sigma_2^y}{2\mu + h_2} \frac{\operatorname{dev} A_2}{|\operatorname{dev} A_2|}$$

and the substitution of this into (15) finally gives the condition

$$\operatorname{dev} A_1 - 2\mu \left(\frac{|\operatorname{dev} A_2| - \sigma_2^y}{2\mu + h_2} \frac{\operatorname{dev} A_2}{|\operatorname{dev} A_2|} \right) \in \sigma_1^y B$$

Case 3: $P_1 \neq 0$, $P_2 = 0$. The same technique as in Case 2, only with the reversed indices 1 and 2, gives

$$P_1 = \frac{|\operatorname{dev} A_1| - \sigma_1^y}{2\mu + h_1} \frac{\operatorname{dev} A_1}{|\operatorname{dev} A_1|}$$

$$\operatorname{dev} A_2 - 2\mu \left(\frac{|\operatorname{dev} A_1| - \sigma_1^y}{2\mu + h_1} \frac{\operatorname{dev} A_1}{|\operatorname{dev} A_1|} \right) \in \sigma_2^y B$$

Case 4: $P_1 \neq 0$, $P_2 \neq 0$ implies

$$\begin{pmatrix} \operatorname{dev} A_1 \\ \operatorname{dev} A_2 \end{pmatrix} - \begin{pmatrix} (2\mu + h_1)\mathbb{I} & 2\mu\mathbb{I} \\ 2\mu\mathbb{I} & (2\mu + h_2)\mathbb{I} \end{pmatrix} \begin{pmatrix} P_1 \\ P_2 \end{pmatrix} = \begin{pmatrix} \sigma_1^y \frac{P_1}{|P_1|} \\ \sigma_2^y \frac{P_2}{|P_2|} \end{pmatrix} \tag{17}$$

Applying substitutions $P_i = \xi_i X_i$, where $|X_i| = 1, i = 1, 2$, (17) becomes a system of non-linear equations with positive parameters $\xi_1 = |P_1|, \xi_2 = |P_2|$, namely

$$\begin{pmatrix} \operatorname{dev} A_1 \\ \operatorname{dev} A_2 \end{pmatrix} = \begin{pmatrix} (\sigma_1^y + (2\mu + h_1)\xi_1)\mathbb{I} & 2\mu\xi_2\mathbb{I} \\ 2\mu\xi_1\mathbb{I} & (\sigma_2^y + (2\mu + h_2)\xi_2)\mathbb{I} \end{pmatrix} \begin{pmatrix} X_1 \\ X_2 \end{pmatrix}$$

Additional substitutions $\eta_1 := \sigma_1^y + (2\mu + h_1)\xi_1$, $\eta_2 := \sigma_2^y + (2\mu + h_2)\xi_2$, $v_1 := 2\mu\xi_1$, $v_2 := 2\mu\xi_2$ and the fact that

$$\begin{pmatrix} \eta_1\mathbb{I} & v_2\mathbb{I} \\ v_1\mathbb{I} & \eta_2\mathbb{I} \end{pmatrix}^{-1} = \frac{1}{\eta_1\eta_2 - v_1 v_2} \begin{pmatrix} \eta_2\mathbb{I} & -v_2\mathbb{I} \\ -v_1\mathbb{I} & \eta_1\mathbb{I} \end{pmatrix}$$

yield

$$\begin{aligned} \eta_2 \operatorname{dev} A_1 - v_2 \operatorname{dev} A_2 &= (\eta_1\eta_2 - v_1 v_2)X_1 \\ -v_1 \operatorname{dev} A_1 + \eta_1 \operatorname{dev} A_2 &= (\eta_1\eta_2 - v_1 v_2)X_2 \end{aligned} \tag{18}$$

Normalization of (18) and the application of substitutions for η_1, η_2, v_1, v_2 give the system of non-linear equations for positive ξ_1, ξ_2

$$|l_1(\xi_1)| - |r(\xi_1, \xi_2)| = 0, \quad |l_2(\xi_2)| - |r(\xi_1, \xi_2)| = 0 \tag{19}$$

where

$$\begin{aligned} l_1(\xi_1) &= (\sigma_1^y + (2\mu + h_1)\xi_1) \operatorname{dev} A_2 - 2\mu\xi_1 \operatorname{dev} A_1 \\ l_2(\xi_2) &= (\sigma_2^y + (2\mu + h_2)\xi_2) \operatorname{dev} A_1 - 2\mu\xi_2 \operatorname{dev} A_2 \\ r(\xi_1, \xi_2) &= (\sigma_1^y + (2\mu + h_2)\xi_1)(\sigma_2^y + (2\mu + h_2)\xi_2) - 4\mu^2\xi_1\xi_2 \end{aligned}$$

Instead of the solving (19) we prefer to solve the equivalent system of non-linear equations

$$\Phi_j(\xi_1, \xi_2) = |l_j(\xi_j)|^2 - (r(\xi_1, \xi_2))^2 = 0, \quad \text{for } j = 1, 2 \tag{20}$$

Lemma 5
Given σ_1^y, σ_2^y, h_1, h_2, μ, $\operatorname{dev} A_1$, $\operatorname{dev} A_2$. Then the solution ξ_2 of the non-linear system (20) is a root of the 8th degree polynomial of the form

$$\begin{aligned} &(J^4F^2)\xi_2^8 + (2T_4J^2F)\xi_2^7 + (2T_3J^2F + T_4^2)\xi_2^6 + (2T_2J^2F + 2T_3T_4)\xi_2^5 \\ &\quad + (2T_1J^2F + 2T_2T_4 + T_3^2 - F(BJ + 2IC)^2)\xi_2^4 \\ &\quad + (-E(BJ + 2IC)^2 - 2F(2CG + BH)(BJ + 2IC) + 2T_1T_4 + 2T_2T_3)\xi_2^3 \end{aligned}$$

$$
\begin{aligned}
&+(-D(BJ+2IC)^2-2E(2CG+BH)(BJ+2IC)-F(2CG+BH)^2\\
&+2T_1T_3+T_2^2)\xi_2^2\\
&+(-2D(2CG+BH)(BJ+2IC)-E(2CG+BH)^2+2T_1T_2)\xi_2\\
&+(T_1^2-D(2CG+BH)^2)=0
\end{aligned}
$$

with the coefficients A, B, C, D, E, F, G, H, I, J defined in the proof below and

$$
\begin{aligned}
T_1 &:= H^2D-CG^2-AH^2-BGH-CD\\
T_2 &:= -BGJ-2HJA-CE-2ICG+H^2E-IBH+2HJD\\
T_3 &:= -CF-J^2A+2HJE-IBJ+C+J^2D+H^2F\\
T_4 &:= 2HJF+J^2E
\end{aligned}
$$

Then

$$
\xi_1=\frac{-I\xi_2-G\pm\sqrt{D+E\xi_2+F\xi_2^2}}{H+J\xi_2}
$$

Proof
Direct calculations reveal

$$
\begin{aligned}
|l_1(\xi_1)|^2 &= |((2\mu+h_1)\operatorname{dev}A_2-2\mu\operatorname{dev}A_1)\xi_1+\sigma_1^y\operatorname{dev}A_2|^2\\
&= |\sigma_1^y\operatorname{dev}A_2|^2+2(\sigma_1^y\operatorname{dev}A_2):((2\mu+h_1)\operatorname{dev}A_2-2\mu\operatorname{dev}A_1)\xi_1\\
&\quad +|(2\mu+h_1)\operatorname{dev}A_2-2\mu\operatorname{dev}A_1|^2\xi_1^2 := A+B\xi_1+C\xi_1^2\\
|l_2(\xi_2)|^2 &= |((2\mu+h_2)\operatorname{dev}A_1-2\mu\operatorname{dev}A_2)\xi_2+\sigma_2^y\operatorname{dev}A_1|^2\\
&= |\sigma_2^y\operatorname{dev}A_1|^2+2(\sigma_2^y\operatorname{dev}A_1):((2\mu+h_2)\operatorname{dev}A_1-2\mu\operatorname{dev}A_2)\xi_2\\
&\quad +|((2\mu+h_2)\operatorname{dev}A_1-2\mu\operatorname{dev}A_2)|^2\xi_2^2 := D+E\xi_2+F\xi_2^2\\
r(\xi_1,\xi_2)^2 &= (\sigma_1^y\sigma_2^y+(2\mu+h_1)\sigma_2^y\xi_1+(2\mu+h_2)\sigma_1^y\xi_2+(2\mu(h_1+h_2)+h_1h_2)\xi_1\xi_2)^2\\
&= (G+H\xi_1+I\xi_2+J\xi_1\xi_2)^2
\end{aligned}
$$

Then Φ_1, Φ_2 are polynomials of the second degree in two variables ξ_1, ξ_2

$$
\begin{aligned}
\Phi_1(\xi_1,\xi_2) &= A+B\xi_1+C\xi_1^2-(G+H\xi_1+I\xi_2+J\xi_1\xi_2)^2=0\\
\Phi_2(\xi_1,\xi_2) &= D+E\xi_2+F\xi_2^2-(G+H\xi_1+I\xi_2+J\xi_1\xi_2)^2=0
\end{aligned}
$$

Expressing ξ_1 from the latter equation and a substitution into the former lead (with MAPLE 5, recently MAPLE 8 could not reproduce this result) to the polynomial (5). □

Example 3.1

Let $\mu=1$, $\sigma_1^y=1$, $\sigma_2^y=2$, $h_1=1$, $h_2=1$ and $A_1=A_2=\begin{pmatrix}20 & 0\\ 0 & 0\end{pmatrix}$. The direct calculation shows

$$l_1(\xi_1)=\begin{pmatrix}10+10\xi_1 & 0\\ 0 & -10-10\xi_1\end{pmatrix}$$

$$l_2(\xi_2)=\begin{pmatrix}20+10\xi_2 & 0\\ 0 & -20-10\xi_2\end{pmatrix}$$

$$r(\xi_1,\xi_2)=5\xi_1\xi_2+6\xi_1+3\xi_2+2$$

and the non-linear system of Equations (20) for positive ξ_1, $\xi_2>0$ reads

$$\Phi_1(\xi_1,\xi_2)=200+400\xi_1+200\xi_1^2-(2+3\xi_2+6\xi_1+5\xi_1\xi_2)^2=0 \tag{21}$$

$$\Phi_2(\xi_1,\xi_2)=800+800\xi_2+200\xi_2^2-(2+3\xi_2+6\xi_1+5\xi_1\xi_2)^2=0 \tag{22}$$

The unknown ξ_1 is expressed from (22)

$$\xi_1=\frac{-3\xi_2-2\pm 10\sqrt{10}(2+\xi_2)}{5\xi_2+6} \tag{23}$$

and the substitution of the plus term into (21) implies after the factorization the equality

$$\frac{(5\xi_2+8-10\sqrt{2})(5\xi_2+4-10\sqrt{2})(\xi_2+2)^2}{(6+5\xi_2)}=0 \tag{24}$$

Note that the substitution of the minus term (23) into (21) leads to the different signs of ξ_1 and ξ_2. The roots of (24) are given by

$$\xi_2=\{-\tfrac{4}{5}+2\sqrt{2},-\tfrac{8}{5}-2\sqrt{2},-2,-2\}$$

There is one positive root $\xi_2=-\frac{4}{5}+2\sqrt{2}\approx 2.028427124$ only, whose substitution into (21) represents the quadratic equation $(995\xi_1+801-50\sqrt{2})(5\xi_1-1-10\sqrt{2})=0$ with roots

$$\xi_1=\left\{-\frac{1}{5}\,\frac{-1+40\sqrt{2}}{1+10\sqrt{2}},\frac{1}{5}\,\frac{201+2\sqrt{2}}{1+10\sqrt{2}}\right\}$$

Merely the first root $\xi_1=-(1/5)(-1+40\sqrt{2})/(1+10\sqrt{2})\approx 3.028427125$ is positive.

3.5. Iterative solution of the discrete inequality

The following iterative scheme is shown to converge towards the solution of the discrete inequality for the two-yield model.

Algorithm 3.2 (*Iterative approach for calculation of* P_1, P_2)
Input μ, h_1, h_2, σ_1^y, σ_2^y, $\operatorname{dev} A_1$, $\operatorname{dev} A_2$ and $\mathrm{tol} \geqslant 0$.

(a) Choose an initial approximation $(P_1^0, P_2^0) \in \operatorname{dev} \mathbb{R}_{\mathrm{sym}}^{d\times d} \times \operatorname{dev} \mathbb{R}_{\mathrm{sym}}^{d\times d}$, set $i := 0$.
(b) Find $P_2^{i+1} \in \operatorname{dev} \mathbb{R}_{\mathrm{sym}}^{d\times d}$ such that

$$f(P_1^i, P_2^{i+1}) = \min_{Q \in \operatorname{dev} \mathbb{R}_{\mathrm{sym}}^{d\times d}} f(P_1^i, Q)$$

(c) Find $P_1^{i+1} \in \operatorname{dev} \mathbb{R}_{\mathrm{sym}}^{d\times d}$ such that

$$f(P_1^{i+1}, P_2^{i+1}) = \min_{Q \in \operatorname{dev} \mathbb{R}_{\mathrm{sym}}^{d\times d}} f(Q, P_2^{i+1})$$

(d) If $|P_1^{i+1}|+|P_1^i|+|P_2^{i+1}|+|P_2^i| = 0$ or $\frac{|P_1^{i+1}-P_1^i|+|P_2^{i+1}-P_2^i|}{|P_1^{i+1}|+|P_1^i|+|P_2^{i+1}|+|P_2^i|} < \mathrm{tol}$ output (P_1^{i+1}, P_2^{i+1}) otherwise set $i := i+1$ and goto (b).

Algorithm 3.2 belongs to the class of alternating direction algorithms. Similarly as in the single-yield case, the minimization problems in steps (b) and (c) can be solved explicitly as

$$P_2^{i+1} = \frac{(|\operatorname{dev} A_2 - 2\mu P_1^i| - \sigma_2^y)_+}{2\mu + h_2} \frac{\operatorname{dev} A_2 - 2\mu P_1^i}{|\operatorname{dev} A_2 - 2\mu P_1^i|}$$

$$P_1^{i+1} = \frac{(|\operatorname{dev} A_1 - 2\mu P_2^{i+1}| - \sigma_1^y)_+}{2\mu + h_1} \frac{\operatorname{dev} A_1 - 2\mu P_2^{i+1}}{|\operatorname{dev} A_1 - 2\mu P_2^{i+1}|}$$

Proposition 1 states the geometrical convergence of Algorithm 3.2.

Proposition 1 (*Convergence of Algorithm 3.2*)
Let (P_1, P_2) be the minimizer of f and let the sequence $(P_1^i, P_2^i)_{i=0}^{\infty}$ be generated by Algorithm 3.2. Define $q := \gamma/(1+\gamma)$, $\gamma := (\min\{\sigma_2^y, \sigma_2^y\})^{-2} L^2 \cdot \alpha^{-2}$, $C_0 := 2(1+\gamma)\cdot\alpha^{-1}\cdot(f(P_1^0, P_2^0) - f(P_1, P_2))$, where $\alpha > 0$ and $L > 0$ are constants for the strong monotonicity and the Lipschitz continuity of the Fréchet-differential of $\Phi(P) := \frac{1}{2}(\hat{\mathbb{H}} + \hat{\mathbb{C}})P : P - A : P$. Then, for any $i \geqslant 1$ there holds

$$|P_1^i - P_1|^2 + |P_2^i - P_2|^2 \leqslant C_0 q^i$$

Proof
Let us decompose the space of $X := \operatorname{dev}(\mathbb{R}_{\mathrm{sym}}^{d\times d}) \times \operatorname{dev}(\mathbb{R}_{\mathrm{sym}}^{d\times d})$ as $X = X_1 + X_2$,

$$X_1 := \{(P_1, 0) : P_1 \in \operatorname{dev}(\mathbb{R}_{\mathrm{sym}}^{d\times d})\} \quad \text{and} \quad X_2 := \{(0, P_2) : P_2 \in \operatorname{dev}(\mathbb{R}_{\mathrm{sym}}^{d\times d})\}$$

Let $M_1 : X \to X_1$ and $M_2 : X \to X_2$ be linear mappings defined as

$$M_1(P_1, P_2) := (P_1, 0) \quad \text{and} \quad M_2(P_1, P_2) := (0, P_2)$$

Then we can show that for all subsets $\Lambda \subseteq \{1, 2\}$ and all $P = (P_1, P_2) \in X$ there holds

$$\left| \sum_{\lambda \in \Lambda} M_\lambda(P_1, P_2) \right| \leqslant (\min\{\sigma_1^y, \sigma_2^y\})^{-1} |(P_1, P_2)|$$

We decompose the functional f as the sum of functional Φ and ψ, where

$$\Phi(P) := \tfrac{1}{2}(\hat{\mathbb{H}} + \hat{\mathbb{C}})P : P - A : P \quad \text{and} \quad \psi(P) := |P|_{\sigma^y} = \sigma_1^y |P_1| + \sigma_2^y |P_2|$$

One can show that the functional Φ is Fréchet-differentiable and $D\Phi$ is strongly monotone with a constant $\alpha > 0$ and Lipschitz continuous with a constant $L > 0$. The convex, lower-semicontinuous functional ψ is additive with respect to the partition $X = X_1 + X_2$, i.e. in the sense that, for all $(x_1, x_2) \in X_1 \times X_2$,

$$\psi(x_1 + x_2) = \psi(x_1) + \psi(x_2)$$

For all $j \in \{1,2\}$, for all $y_j \in \sum_{k=1,k\neq j}^{2} X_k$, there holds $M_j y_j = 0$ and therefore for all $x_j \in X_j$ holds

$$\psi(x_j + M_j y_j) = \psi(x_j)$$

thus ψ is also independent with respect to the partition $X = X_1 + X_2$. Estimate (1) is then an immediate consequence of Theorem 2.1 in Reference [9]. □

The next example illustrates the behaviour of Algorithm 3.2.

Example 3.2

Let $\mu = 1$, $\sigma_1^y = 1$, $\sigma_2^y = 2$, $h_1 = 1$, $h_2 = 1$, $A_1 = A_2 = \begin{pmatrix} 20 & 0 \\ 0 & 0 \end{pmatrix}$, tol$=10^{-12}$ and the initial approximation

$$P_2^0 = \frac{(|\operatorname{dev} A_2| - \sigma_2^y)_+}{2\mu + h_2} \frac{\operatorname{dev} A_2}{|\operatorname{dev} A_2|}, \quad P_1^0 = \frac{(|\operatorname{dev} A_1 - 2\mu P_2^0| - \sigma_1^y)_+}{2\mu + h_1} \frac{\operatorname{dev} A_1 - 2\mu P_2^0}{|\operatorname{dev} A_1 - 2\mu P_2^0|}$$

Algorithm 3.2 generates approximations P_1^i, P_2^i, $i = 1, 2, \ldots$ in the form

$$P_1^i = \begin{pmatrix} x^i & 0 \\ 0 & -x^i \end{pmatrix} \quad \text{and} \quad P_2^i = \begin{pmatrix} y^i & 0 \\ 0 & -y^i \end{pmatrix}$$

and terminates after 34 approximations with

$$P_1^{34} = \begin{pmatrix} 2.14142 & 0 \\ 0 & -2.14142 \end{pmatrix} \quad \text{and} \quad P_2^{34} = \begin{pmatrix} 1.43431 & 0 \\ 0 & -1.4343 \end{pmatrix}$$

Figure 1 displays the approximations (P_1^i, P_2^i), $i = 0, 1, 2, \ldots, 34$ as the points (x^i, y^i) in the x–y co-ordinate system. Note that values $\|P_1^{34}\| \approx 3.028425$ and $\|P_2^{34}\| \approx 2.0284207$ correspond to values of ξ_1 and ξ_2 calculated in Example 3.1.

4. NUMERICAL EXPERIMENTS

Three numerical simulations illustrate the algorithms of this paper. More can be found in References [10,11].

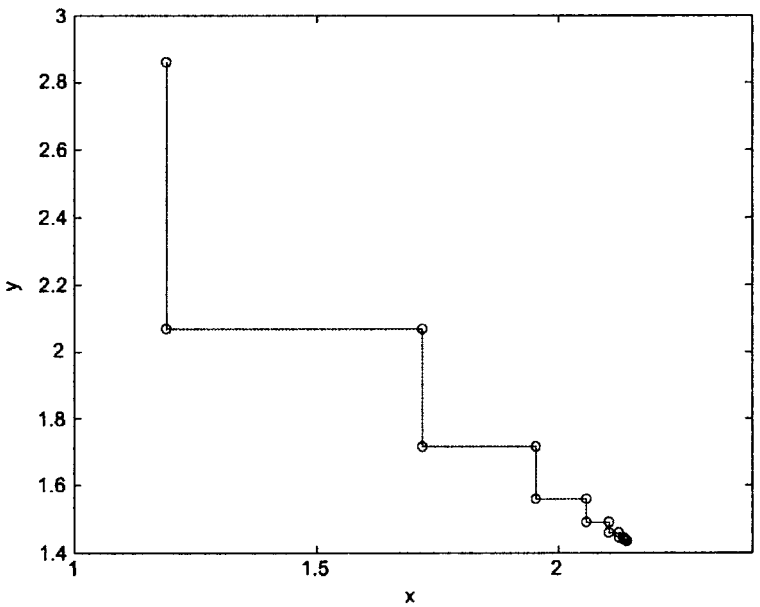

Figure 1. The approximations $P_1^i = (x^i, 0; 0, -x^i)$, $P_2^i = (y^i, 0; 0, -y^i)$, $i = 0, \ldots, 34$ computed by Algorithm 3.2 in Example 3.2 and displayed as the points (x^i, y^i) in the x–y co-ordinate system.

4.1. 1D beam

To illustrate 1D effects, we study the following beam problem as displayed in Figure 3 (left). We consider the unit square shape $\Omega = (0,1)^2$ in a x–y co-ordinate system with the following boundary conditions for the displacement $u := (u_1, u_2)$ and the surface force g:

$$\begin{aligned} &u(0,y) = (0,u_2) \quad \text{for } 0 < y \leqslant 1, \quad u(0,0) = (0,0) \\ &g(x,0) = g(x,1) = (0,0) \quad \text{for } 0 < x < 1 \\ &g(1,y) = (g_1, 0) \quad \text{for } 0 \leqslant y \leqslant 1 \end{aligned} \tag{25}$$

with a given constant $g_1 \in \mathbb{R}$. Because of symmetries in the boundary conditions, the beam displacement $u = (u_1(x,y), u_2(x,y))$ can be expected in the form

$$u(x,y) = (u_1, u_2)(x,y) = (x \cdot u_1(1,0), y \cdot u_2(0,1)) \quad \text{for } (x,y) \in \Omega$$

which implies for the strain tensor

$$\varepsilon(u) = \begin{pmatrix} u_1(1,0) & 0 \\ 0 & u_2(0,1) \end{pmatrix} \quad \text{in } \Omega$$

Besides that, the Neumann boundary conditions (25) admit the stress tensor

$$\sigma = \begin{pmatrix} g_1 & 0 \\ 0 & 0 \end{pmatrix} \quad \text{in } \Omega$$

There holds Hooke's law in the purely elastic phase (no plasticity), $\sigma = 2\mu\varepsilon + \lambda(\operatorname{tr}\varepsilon)\mathbb{I}$, i.e.

$$\begin{pmatrix} g_1 \\ 0 \\ 0 \end{pmatrix} = \begin{pmatrix} 2\mu+\lambda & \lambda & 0 \\ \lambda & 2\mu+\lambda & 0 \\ 0 & 0 & 2\mu \end{pmatrix} \begin{pmatrix} u_1(1,0) \\ u_2(0,1) \\ 0 \end{pmatrix}$$

The inverse rule

$$\begin{pmatrix} 2\mu+\lambda & \lambda & 0 \\ \lambda & 2\mu+\lambda & 0 \\ 0 & 0 & 2\mu \end{pmatrix}^{-1} = \begin{pmatrix} \dfrac{2\mu+\lambda}{4\mu(\mu+\lambda)} & -\dfrac{\lambda}{4\mu(\mu+\lambda)} & 0 \\ -\dfrac{\lambda}{4\mu(\mu+\lambda)} & \dfrac{2\mu+\lambda}{4\mu(\mu+\lambda)} & 0 \\ 0 & 0 & \dfrac{1}{2\mu} \end{pmatrix}$$

implies that the (elastic) deformation of the beam can be expressed as

$$u(x,y)(t) = \left(x\,\frac{2\mu+\lambda}{4\mu(\mu+\lambda)}, -y\,\frac{\lambda}{4\mu(\mu+\lambda)} \right) g_1(t) \tag{26}$$

The shape of solution (26) allows to simulate 1D elastoplastic processes by this 2D model. The numerical experiment for the hysteresis behaviour demonstration was the calculation on the coarse mesh $\mathscr{T}_0$ with 16 elements, discrete times $\{0, 0.5, 1, \ldots, 50\}$, in case of the time-dependent uniform cyclic surface loading $g_1 = 12\,\sin(t\pi/20)$. In order to compare two different material models, we firstly considered the two-yield material specified by parameters $\mu = 1000$, $\lambda = 1000$, $\sigma_1^y = 5$, $h_1 = 100$, $\sigma_2^y = 7$, $h_2 = 50$ and secondly the single-yield material specified by parameters $\mu = 1000$, $\lambda = 1000$, $\sigma^y = 5$, $h = 100$. Figure 4 shows hysteresis curves in terms of the dependence of $g_1(t)$ on the x-displacement $u_1(t)$ of the point $(x = 1, y = 0)$ for the single (left) and two-yield material (right) models.

4.2. 2D beam

In order to take 2D effects into account, we study a second beam problem (Figure 2). Its geometry is identical to the problem of beam with 1D effects, and the only difference being modified is the Dirichlet boundary condition, see Figure 3 (right). We prescribe the Dirichlet boundary Γ_D in both directions (i.e. the beam is fixed in both directions at Γ_D), i.e.

$$u(0,y) = (0,0) \quad \text{for } 0 \leqslant y \leqslant 1$$

The first numerical experiment demonstrates 2D hysteresis effects. Material and time parameters, the shape of the mesh are identical to the numerical experiment for the problem

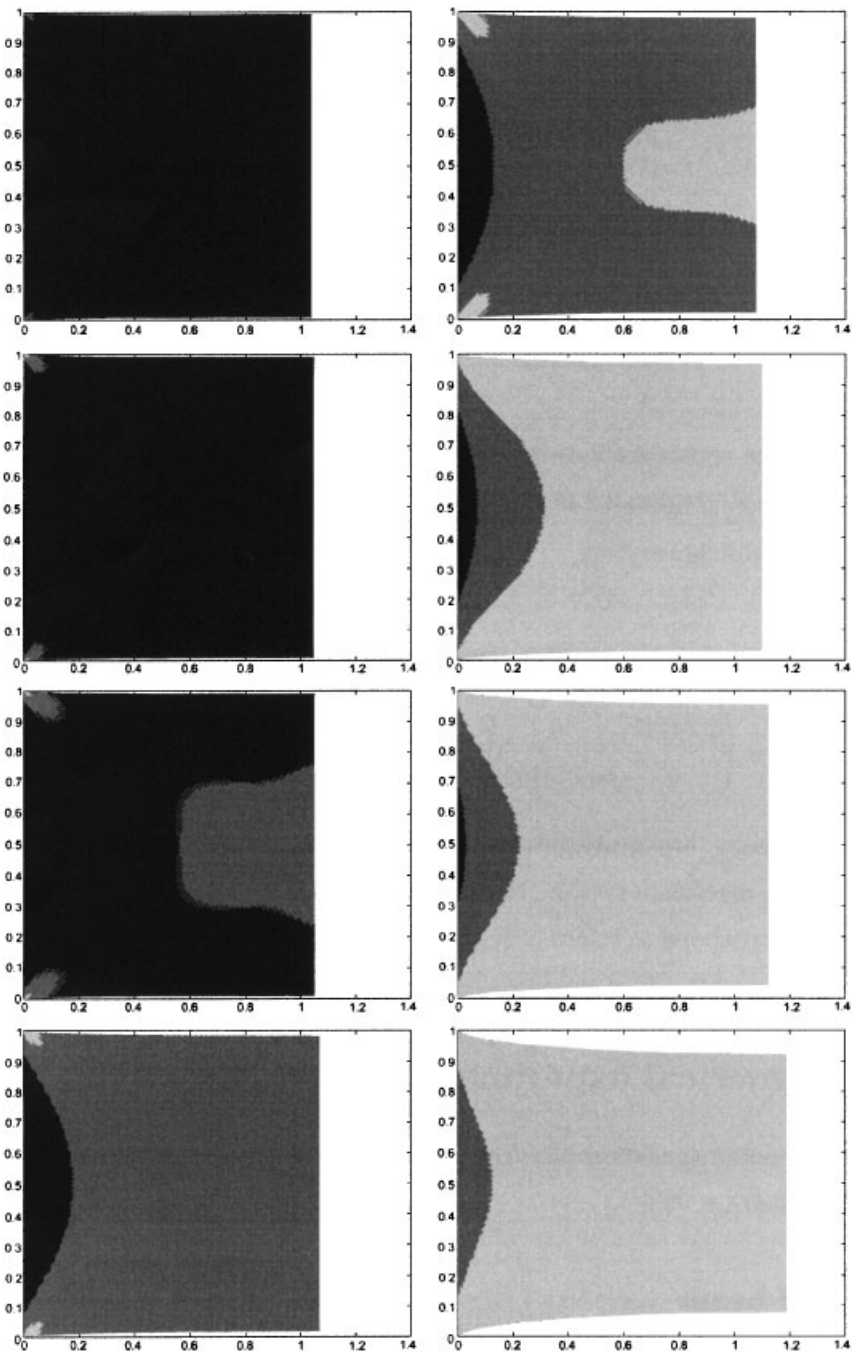

Figure 2. Evolution of elastoplastic zones at discrete times $t = 4.5, 5, 5.5, 6, 6.5, 7, 8, 9$ in the numerical experiment with the two-yield 2D beam explained in Section 4.2. The black colour shows elastic zones, brown and lighter grey colour zones in the first and second plastic phase. A corresponding movie can be found in Reference [4].

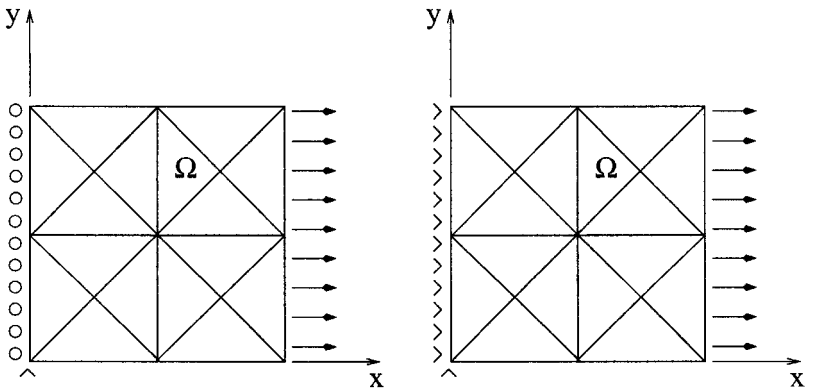

Figure 3. Geometry and coarse mesh $\mathcal{T}_0$ of 1D beam (left) and 2D beam (right).

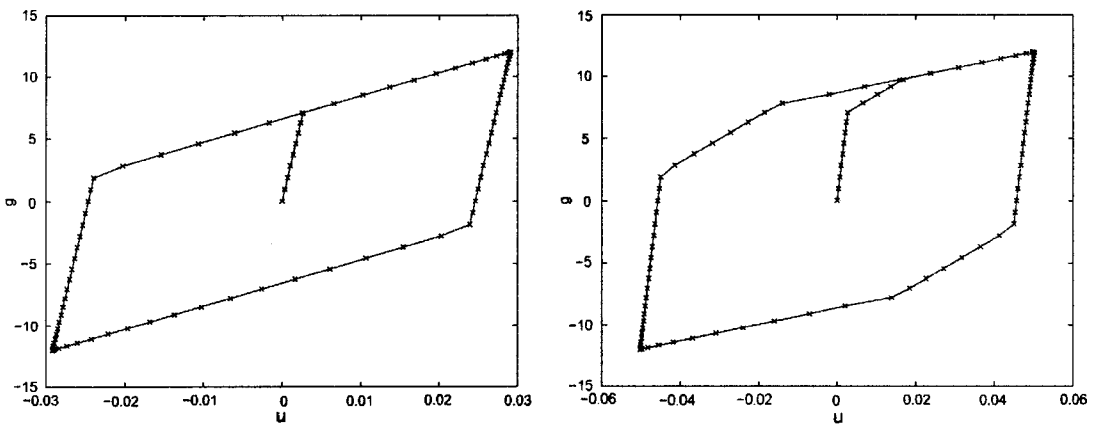

Figure 4. Displayed loading-deformation relation in terms of the uniform surface loading $g_1(t)$ versus the x-displacement of the point (0,1) for problems of the single-yield 1D beam (left) and two-yield 1D beam (right).

of the beam with ID effects. Figure 5 shows the hysteresis curves for the single (left) and the two-yield (right) material. A comparison of Figure 4 with Figure 5 indicates that 2D deformation effects smooth out the elastoplastic transition.

The second numerical experiment describes an elastoplastic transition during the deformation process. The calculation was performed at discrete times $\{0, 0.5, 1, \ldots, 10\}$, applying the uniform surface loading

$$g_1 = t$$

and the same materials as in the first experiment. Figure 2 displays the evolution of elastoplastic zones at chosen discrete times in the deformed configuration. As the deformation

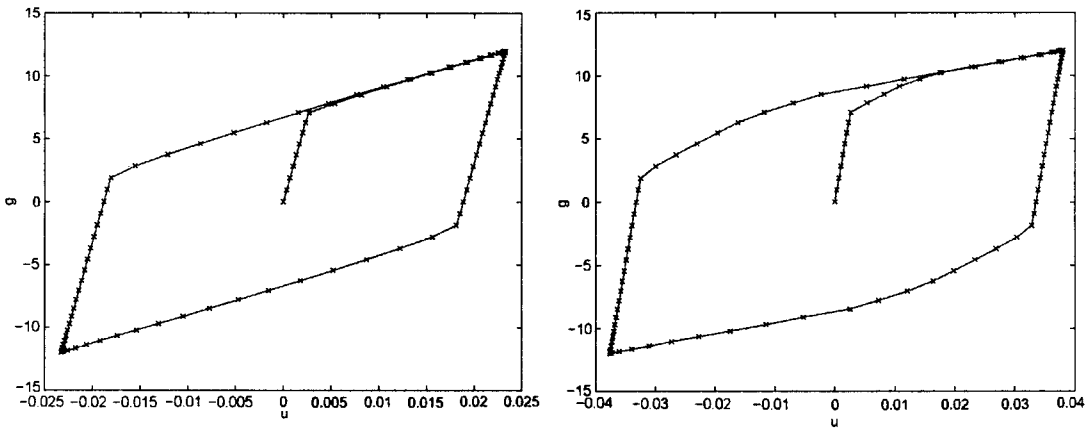

Figure 5. Displayed loading-deformation relation in terms of the uniform surface loading $g_1(t)$ versus the x-displacement of the point (0,1) for problems of the single-yield beam with 2D effects (left) and two-yield beam with 2D effects (right).

process starts (at discrete times $t = \{0, 0.5, \ldots, 4.5\}$), the material behaves purely elastically. At discrete time $t = 5.0$ there appear the first plastic zones in corners (where the material is fixed) and also in the right part of the domain Ω (where external forces g act). For the two-yield model there appear the second plastic zones after the discrete time $t = 5.5$, and they develop in the same way as the first plastic zones at the time $t = 5$. For the final discrete time $t = 10$, both material models are in entirely plastic phases. An animation describing the evolution of this process can be downloaded from Reference [4]. The MATLAB code that was used for the calculation of first two problems can be downloaded from Reference [12].

4.3. 3D crankshaft

The crankshaft model consists of three crank axles and two crank arms linked by four crank disks and is solely loaded by applied surface tractions. Homogeneous Dirichlet boundary conditions are required on the left crank axle and the right crank axle as indicated in Figure 4.3 (top). The surface loads with the value 0.5 in the vertical direction (indicated by arrows in Figure 4.3 (top)) is applied to the cylindrical surfaces of the both crank arms. The middle crank axle surface as well as remaining crank surfaces are traction-free surfaces with zero Neumann boundary condition. The resulting stresses are computed for one time step with zero initial conditions for the two-yield continuum specified by material parameters $E = 1, \nu = 0, \sigma_1^y = 1, h_1 = 1, \sigma_2^y = 1.5, h_2 = 1$ and for the finest uniform mesh with 808 448 tetrahedra obtained by three uniform refinements of the coarse mesh. The calculation took 25 min and was performed by an extension of the elasticity package [13] part of NETGEN/NGSolve software [14] with multigrid preconditioner for the solution of linear system of equations. Figure 4.3 (bottom) displays the resulting three elastoplastic phases on the surfaces. Further details may be found in Reference [11].

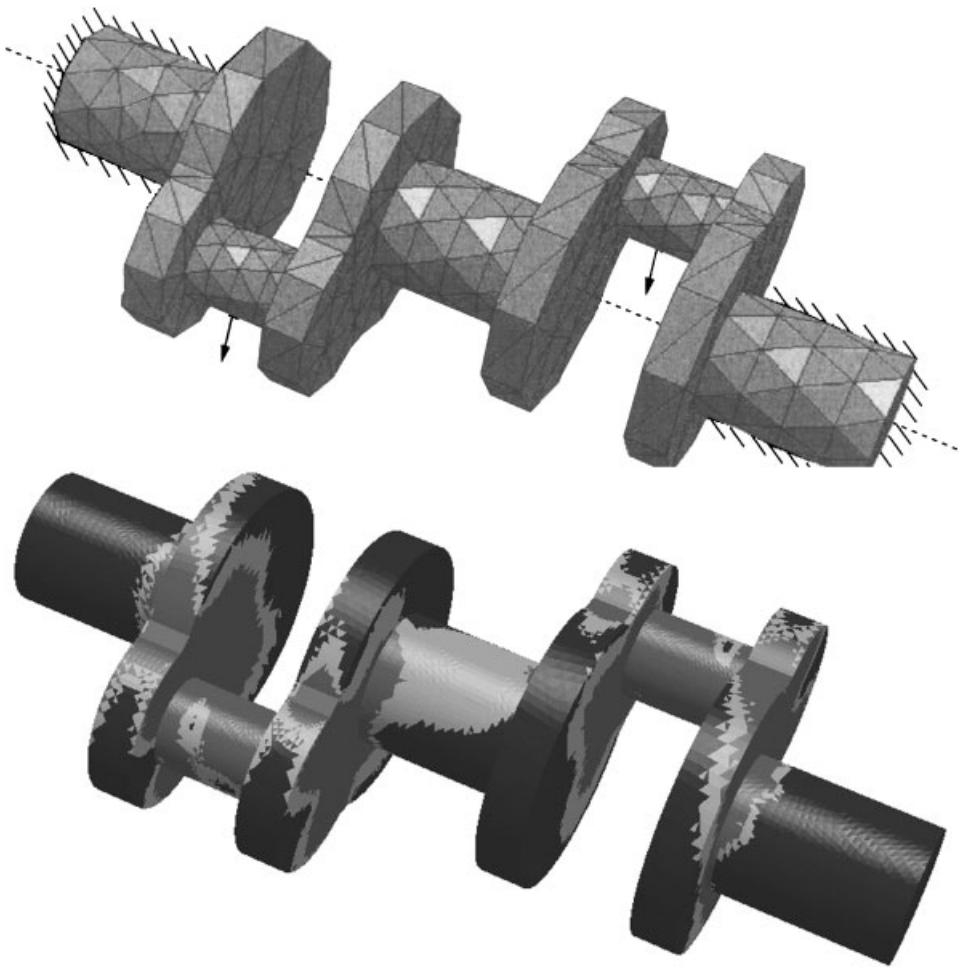

Figure 6. Geometry with the load setup (top) and elastoplastic zones (bottom) in the numerical experiment with the two-yield crankshaft explained in Section 4.3. The black colour shows elastic zones, light and dark grey colour zones in the first and second plastic phase. Pictures were generated by NETGEN/NGSOLVE software [14].

ACKNOWLEDGEMENTS

The authors are pleased to acknowledge support by the German Research Foundation (DFG) through the Graduiertenkolleg 357 'Effiziente Algorithmen und Mehr-skalenmethoden' in Kiel, Germany. The second author was supported by the Forschungszentrum FZ86. The third author acknowledges support from the Austrian Science Fund 'Fonds zur Förderung der wissenschaftlichen Forschung (FWF)' for his support under Grant SFB F013/F1306 in Linz, Austria. The last author acknowledges software support and advise from Dr J. Alberty, J. Kienesberger, and Dr J. Schöberl.

REFERENCES

1. Brokate M, Carstensen C, Valdman J. A quasi-static boundary value problem in multi-surface elastoplasticity: part 1—analysis. *Mathematical Models and Methods in Applied Sciences* 2004; **27**:1697–1710.

2. Han W, Reddy BD. *Plasticity*: *Mathematical Theory and Numerical Analysis*. Springer: New York, 1999.
3. Alberty J, Carstensen C. Numerical analysis of time-depending primal elastoplasticity with hardening. *SIAM Journal on Numerical Analysis* 2000; **37**(4):1271–1294.
4. http://www.sfb013.uni-linz.ac.at/projects/Fl306/beam2d_evolution.gif
5. Ciarlet PG. *The Finite Element Method for Elliptic Problems*. North-Holland: Amsterdam, 1978.
6. Alberty J, Carstensen C, Funken SA, Klose R. Matlab implementation of the finite element method in elasticity. *Computing* 2002; **69**(3):239–263.
7. Hackbusch W. *Multi-Grid Methods and Applications*. Springer: Berlin, Heidelberg, 1985.
8. Alberty J, Carstensen C, Zarrabi D. Adaptive numerical analysis in primal elastoplasticity with hardening. *Computer Methods in Applied Mechanics and Engineering* 1999; **171**(3–4):175–204.
9. Carstensen C. Domain decomposition for a non-smooth convex minimalization problems and its application to plasticity. *Numerical Linear Algebra with Applications* 1997; **4**(3):177–190.
10. Valdman J. Mathematical and numerical analysis of elastoplastic material with multi-surface stress–strain relation. *Ph.D. Thesis*, Christian-Albrechts-Universität zu Kiel, 2002.
11. Kienesberger J, Valdman J. Multi-yield elastoplastic continuum-modeling and computations. In *Numerical Mathematics and Advanced Applications. Proceedings of ENUMATH 2003*, Feistauer M, Dolejší, Knobloch P, Najzar K (eds), Lecture Notes in Computer Science. Springer: Berlin, 2003; 539–548.
12. Valdman J. Two-yield elastoplasticity Matlab solver. Download: http://www.sfb013.uni-linz.ac.at/∼jan/solver.zip
13. Kienesberger J. Multigrid preconditioned solvers for some elastoplastic problems. In *Proceedings of LSSC 2003*, Lirkov I, Margenov S, Waśniewski J, Yalamov P (eds), Lecture Notes in Computer Science, vol. 2907. Springer: Berlin, 2004; 379–386.
14. Schöberl J. Netgen/Ngsolve—mesh generator/3d finite element solver software package. Download: http://www.hpfem.jku.at/netgen/

